ANNALS OF GEOPHYSICS, 68, 1, V107, 2025; doi:10.4401/ag-9155
OPEN ACCESS

APPENDIX TO

METHANA MAGMATIC OBSERVATIONAL EXPERIMENT (MEMAX) – SEISMOLOGICAL MONITORING OF MAGMATIC AND TECTONIC ACTIVITY IN THE WESTERN SARONIC GULF REGION, GREECE

Jan-Phillip Föst[1,2], Joachim R. R. Ritter[2], Christos P. Evangelidis[3], Efthimios Sokos[4], Nicole Richter[1], Klaus R. Reicherter[1]

[1] RWTH Aachen University, Teaching and Research Area Neotectonics and Natural Hazards, Aachen, Germany
[2] Karlsruhe Institute of Technology, Geophysical Institute, Karlsruhe, Germany
[3] National Observatory of Athens, Institute of Geodynamics, Athens, Greece
[4] University of Patras, Laboratory of Seismology, Patras, Greece

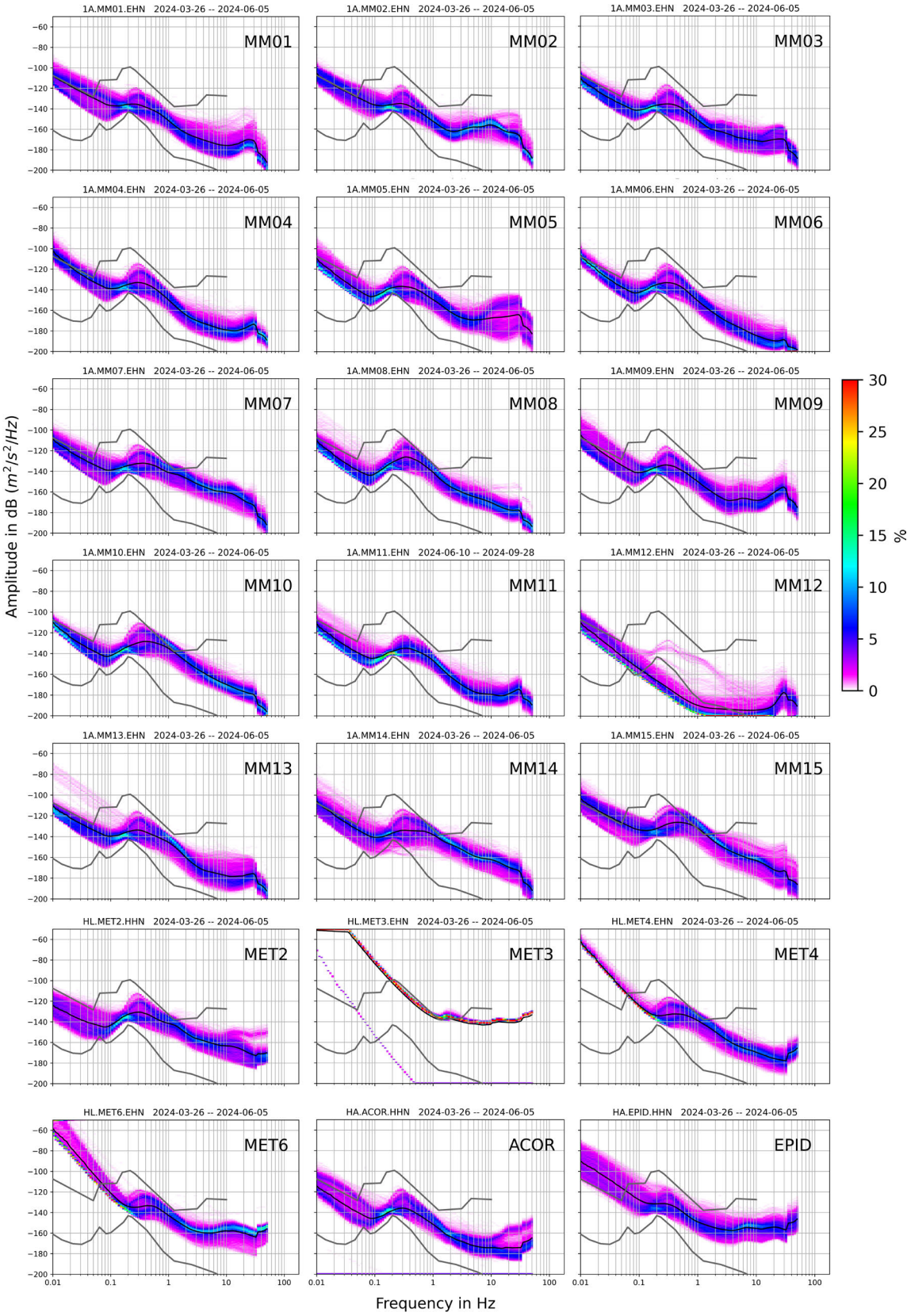

Figure A1. PPSDs for the recording time 26 March-5 June 2024 (until the first service for all stations in the area of MeMaX). The results for the north-south component recordings are presented (for vertical component, see Fig. 6). The PPSDs are calculated for one-hour time windows with an overlap of 50 %. The colour coding represents the spectral power amplitude at a certain frequency. The grey lines show the new high and low noise models (NHNM, NLNM) after Peterson, (1993). The black line indicates the median noise level. Station MM12 had a technical problem, which was fixed end of September 2024.

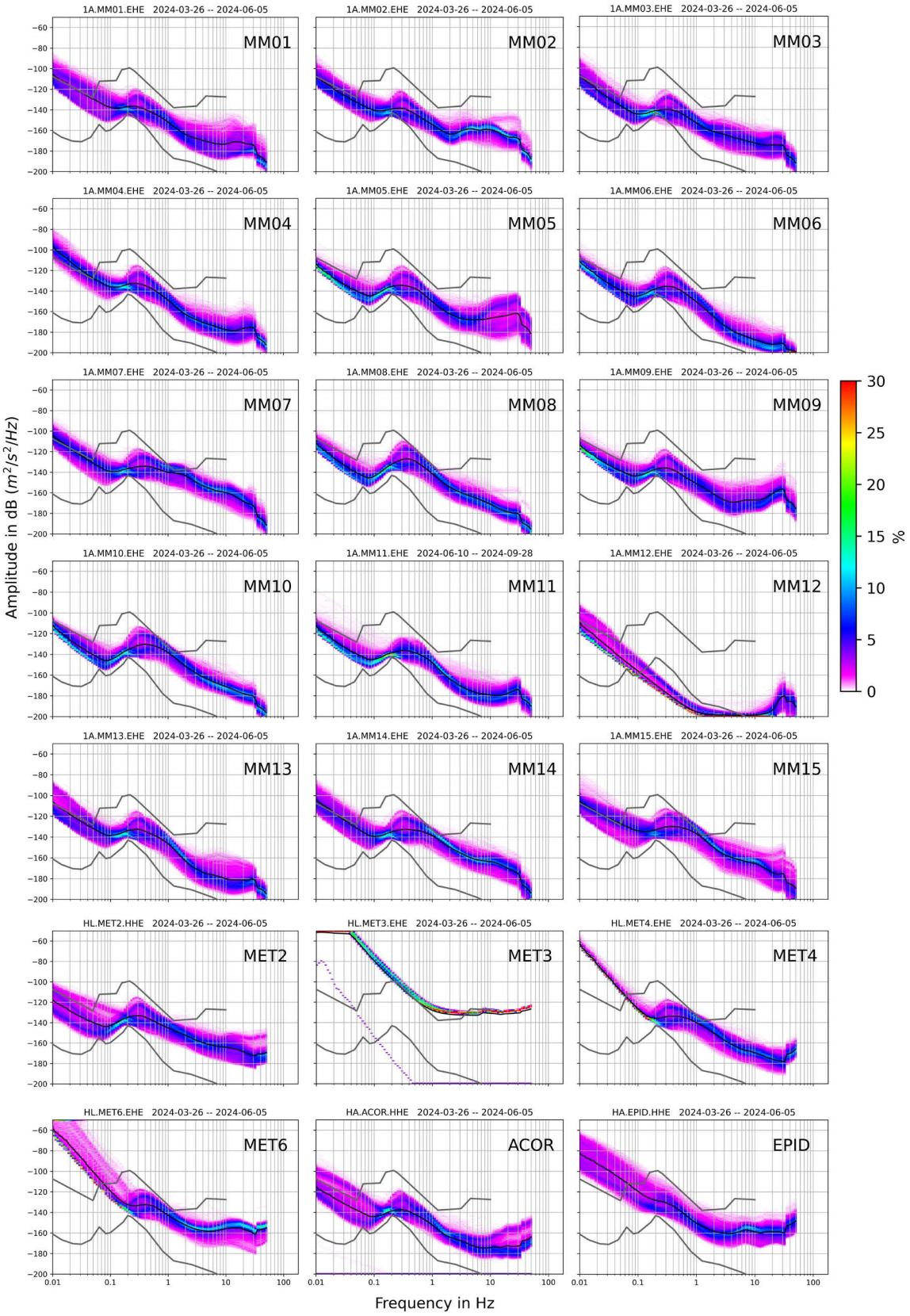

Figure A2. PPSDs for the recording time 26 March-5 June 2024 (until the first service for all stations in the area of MeMaX). The results for the east-west component recordings are presented (for vertical component, see Fig. 6). The PPSDs are calculated for one-hour time windows with an overlap of 50 %. The colour coding represents the spectral power amplitude at a certain frequency. The grey lines show the new high and low noise models (NHNM, NLNM) after Peterson, (1993). The black line indicates the median noise level. Station MM12 had a technical problem, which was fixed end of September 2024.

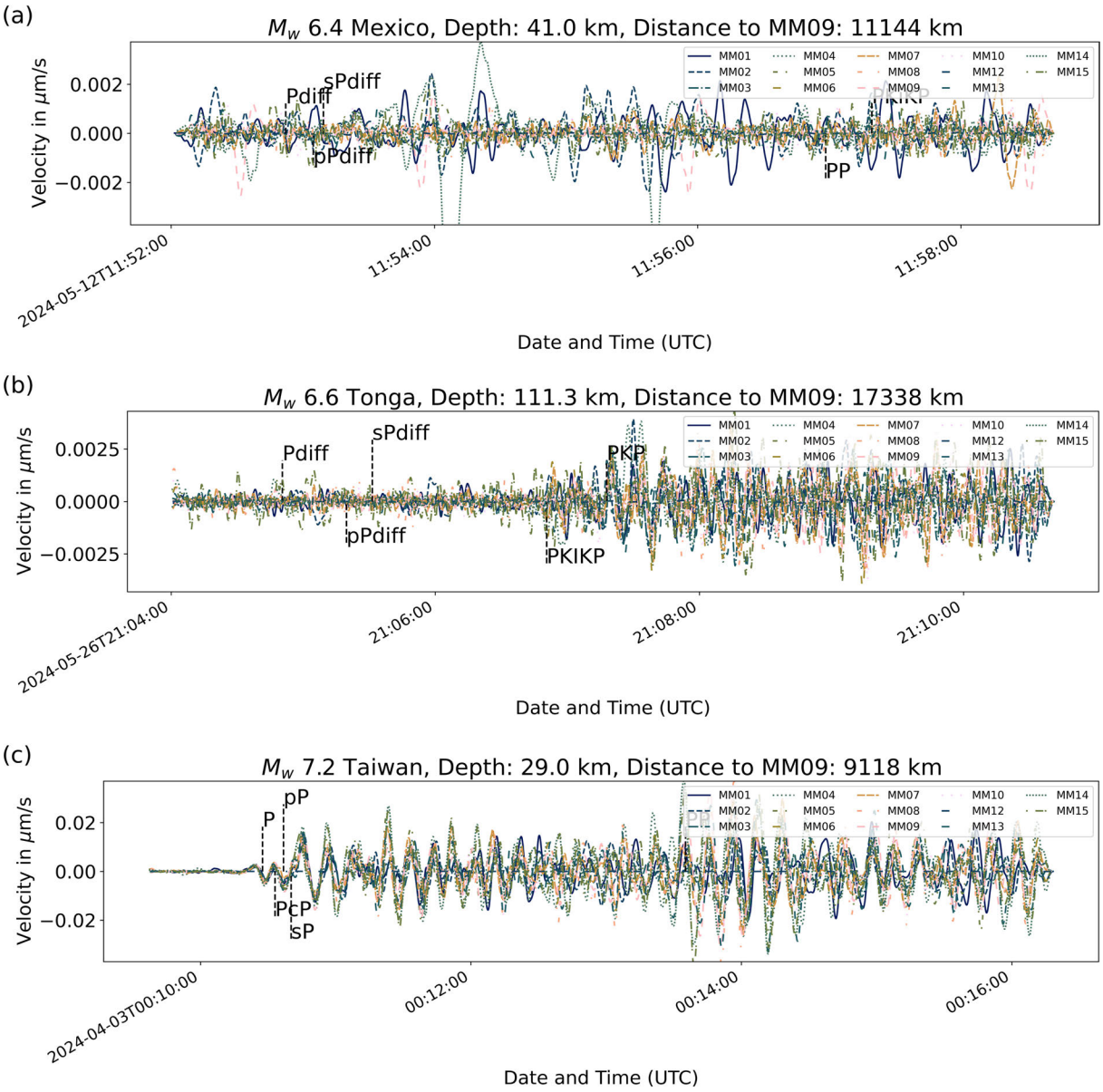

Figure A3. Waveform recordings for three teleseismic earthquakes are presented, showing the north-south components for all stations. The response function is removed to show the actual recording even at very low frequencies (<0.1 Hz), see text. (a) The first arrivals of the *Mw* 6.4 earthquake on 12 June 2024, in Mexico at a depth of 41 km. (b) The first arrival of the *Mw* 6.6 earthquake on 26 June 2024, in Tonga at a depth of 111.3 km. (c) The first arrival of the *Mw* 7.2 earthquake on 3 April 2024, in Taiwan at a depth of 29 km. The recordings are also bandpass filtered with a lower cutoff frequency of 0.01 Hz and an upper cutoff frequency of 0.1 Hz. Linear trends and the mean are subtracted. The theoretical arrival phases are indicated, calculated using TauPy in ObsPy with the ak135 Earth model (Kennett et al., 1995).

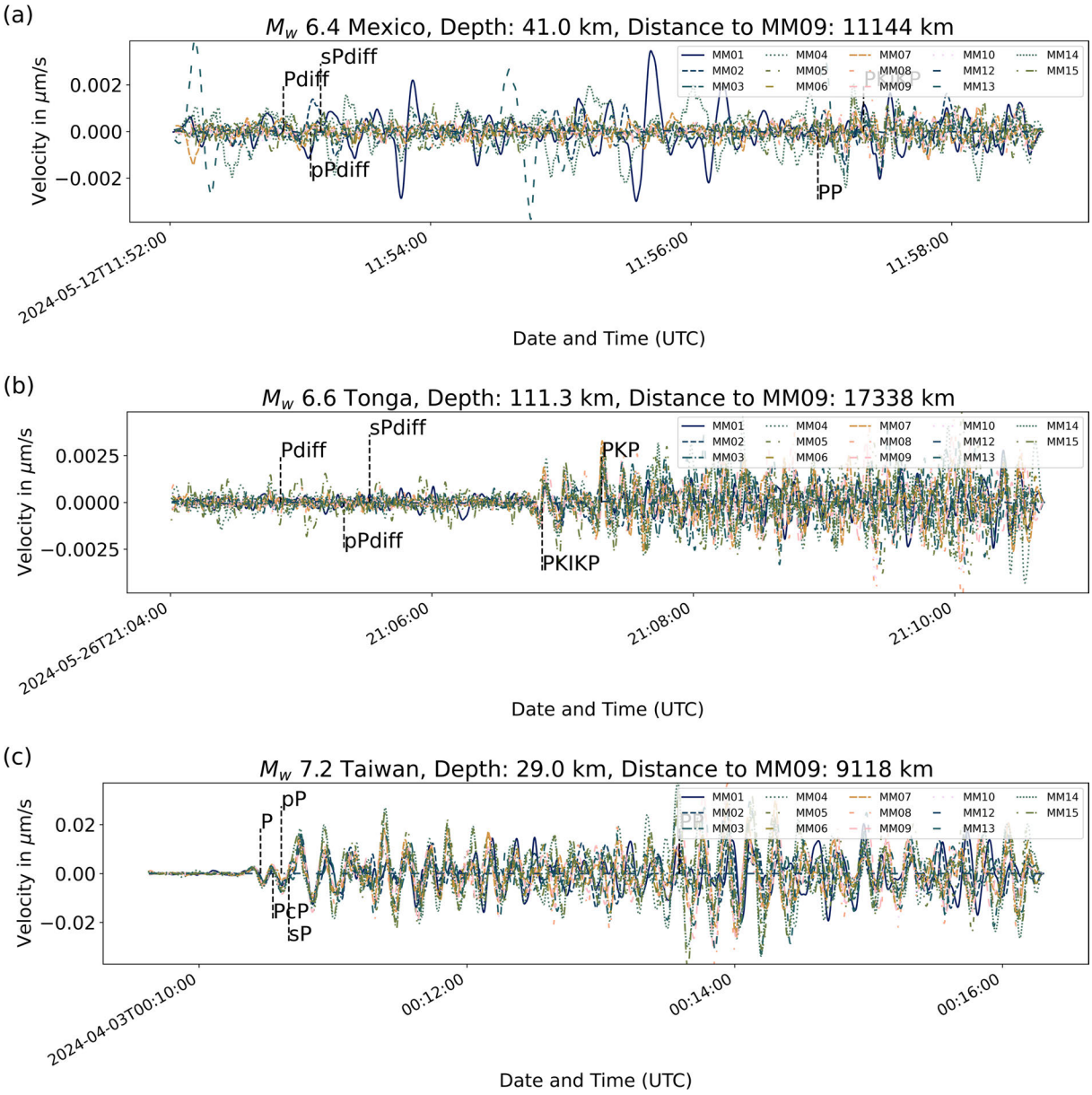

Figure A4. Waveform recordings for three teleseismic earthquakes are presented, showing the east-west channels at all stations. The response function is removed to show the actual recording even at very low frequencies (<0.1 Hz), see text. (a) The first arrivals of the *Mw* 6.4 earthquake on 12 June 2024, in Mexico at a depth of 41 km. (b) The first arrival of the *Mw* 6.6 earthquake on 26 June 2024, in Tonga at a depth of 111.3 km. (c) The first arrival of the *Mw* 7.2 earthquake on 3 April 2024, in Taiwan at a depth of 29 km. The recordings are also bandpass filtered with a lower cutoff frequency of 0.01 Hz and an upper cutoff frequency of 0.1 Hz. Linear trends and the mean are subtracted. The theoretical arrival phases are indicated, calculated using TauPy in ObsPy with the ak135 Earth model (Kennett et al., 1995).